AIAA-99-4034

A Methodology for Evaluating the Fidelity Of Ground-Based Flight Simulators

Y. Zeyada and R. A. Hess
Dept. of Mechanical and Aeronautical Engineering
One Shields Ave.
University of California
Davis, CA 95616-5294

AIAA Modeling and Simulation Conference and Exhibit
9-11 August 1999 / Portland, Oregon

A Methodology for Evaluating the Fidelity of Ground-Based Flight Simulators

Y. Zeyada[1] and R. A. Hess[2]
Dept. of Mechanical and Aeronautical Engineering
One Shields Ave.
University of California
Davis, CA 95616

Abstract

An analytical and experimental investigation was undertaken to model the manner in which pilots perceive and utilize visual, proprioceptive, and vestibular cues in a ground-based flight simulator. The study was part of a larger research effort which has the creation of a methodology for determining flight simulator fidelity requirements as its ultimate goal. The study utilized a closed-loop feedback structure of the pilot/simulator system which included the pilot, the cockpit inceptor, the dynamics of the simulated vehicle and the motion system. With the exception of time delays which accrued in visual scene production in the simulator, visual scene effects were not included in this study. The NASA Ames Vertical Motion Simulator was used in a simple, single-degree of freedom rotorcraft bob-up/down maneuver. Pilot/vehicle analysis and fuzzy-inference identification were employed to study the changes in fidelity which occurred as the characteristics of the motion system were varied over five configurations. The data from three of the five pilots that participated in the experimental study were analyzed in the fuzzy-inference identification. Results indicate that both the analytical pilot/vehicle analysis and the fuzzy-inference identification can be used to reflect changes in simulator fidelity for the task examined.

Acknowledgement

The research described has been supported under a NASA Ames - UC Davis Joint Research Interchange NCC2-5238. The NASA researchers involved were Mr. William Chung (now with Logicon-Syre Corp), Dr. Jeffrey Schroeder and Mr. Duc Tran.

Introduction and Background

Validating the fidelity of ground-based flight simulators is a problem of continuing interest to the simulation community. The ultimate objective of the research to be described is the development of a procedure for determining simulation requirements that will ensure acceptable fidelity. The need for such requirements can be clearly seen from Fig. 1, taken from Ref. 1. Here a comparison is made between the Cooper-Harper pilot opinion ratings obtained from flight test and moving-base simulator evaluations for a group of low-speed rotorcraft maneuvers. As the figure indicates, there exists a significant difference between the ratings given in flight and simulation, indicating shortcomings in the fidelity of the simulator. An analytical approach to addressing some of these problems was discussed in Refs. 2 and 3.

The approach to be discussed builds upon the work of Refs. 2 and 3 and utilizes a model of the pilot's perceptual and response characteristics as captured in the Structural Pilot Model discussed in Ref. 4. In addition, fuzzy-inference identification of human pilot behavior is exploited. While the use of fuzzy-inference models to describe human control behavior is not new, e.g., Refs. 5 and 6, to the authors' knowledge this is the first time they have been employed in simulator fidelity studies.

The Experiment

A pilot-in-the-loop simulation of a rotorcraft bob-up/down maneuver using the NASA Ames Vertical Motion Simulator (VMS) provides the data base for the study. Details of this simulation can be found in Ref. 7. A simplified rotorcraft model was

[1]Postgraduate Researcher

[2]Professor and Vice Chairman, Associate Fellow, AIAA

employed in the simulation study with the characteristics of the motion and visual systems serving as the experimental variables. Table 1 describes the vehicle model and the subset of the motion system dynamics investigated herein. The task consisted of a bob-up from a stabilized hover to a target 32 ft from the initial rotorcraft position, a stabilized hover, then a bob-down to the original position. Figure 2 is a representation of the geometry of the task. Constraints were placed upon the translation time to ensure aggressive pilot behavior. Task performance standards are given in Table 2. Five pilots were used in the experiment and the data from the first three of the pilots involved in the simulation were analyzed here. For the purposes of this study, the important experimental results were the subjective pilot Cooper-Harper handling qualities ratings (HQRs), pilot-induced oscillation ratings (PIORs) and motion fidelity ratings (MFRs).[7] The scales describing these ratings are shown in Figs. 3-5. Table 3 summarizes the pilot rating data for all the three pilots whose data was analyzed in this study. The "Average Composite Score" shown in Table 3 was an attempt to obtain an average numerical score reflecting the HQR, PIOR and MFR for all three pilots values. The score was calculated as follows:

Average Composite Score for Config."j" =

$$\frac{\sum_{i=1}^{3}(HQR_i)_j+\sum_{i=1}^{3}(PIOR_i)_j\cdot\frac{10}{6}+\sum_{1}^{3}\frac{10}{(MFR_i)_j}}{\min_{all\ j}\left[\sum_{i=1}^{3}(HQR_i)_j+\sum_{i=1}^{3}(PIOR_i)_j\cdot\frac{10}{6}+\sum_{1}^{3}\frac{10}{(MFR_i)_j}\right]} \quad (1)$$

The factors 10/6 and 10 applied to the PIOR and 1/MFR ratings means that the worst Cooper-Harper rating, worst PIO rating and worst fidelity rating would make equal contributions of 10 to the numerator of Eq. 1. In contrast the best ratings would make respective contributions of 1, 1 and 3.33. The authors aware of the danger of mixing handling qualities, PIO and simulator fidelity ratings as suggested in Eq. 1. However, the resulting composite scoring approach was felt to be justified here given the fact that a single-axis task was involved, only a single experimental variable, the motion system dynamics, were varied and that these dynamics were systematically degraded from Config. V1 in Table 1.

Pilot/Vehicle Analysis

Loop Structure

Figure 6 is a block diagram representation of the Structural Model of the human pilot used in the study. This model forms the assumed pilot compensation in the inner-most "primary control loop", i.e. that loop that forms the inner-most *visual* control loop.[2,3] The model was implemented in a MATLAB-based computer-aided-design packaged referred to as PVD_{NL}.[8] Figure 7 is a block diagram of the complete pilot/vehicle system, with the structural model forming Y_{p_h}. Thus, an inner, vertical-velocity loop is assumed to serve as the primary control loop. The inner-loop crossover frequency is selected as 2.0 rad/s, as required in the handling qualities assessment technique of Ref. 4. The loop-closure sequence is based upon the fact that the inner, vertical-velocity loop can be closed with gain-like pilot compensation, and the required visual cue, vertical velocity can be sensed relatively easily by the pilot in the experimental setup.

The outer-loop closure consists of feeding back vertical height error, again a variable that can be easily sensed by the pilot in the experiment. The outer loop compensation is a simple gain, i.e., $Y_{p_h} = K_h$. The separation between the inner and outer-loop crossover frequencies was selected as a factor of 3. Thus the outer, height loop is closed at 0.667 rad/s.

Modeling the Inceptor

For the bob-up/down maneuvers that were the subject of this experiments and analysis, the cockpit inceptor was the main rotor collective control. The "force/feel" characteristics of the device are significantly different from those of most cockpit inceptors in that there is no self-centering characteristics and there is significant and deliberate friction introduced in the device's dynamics, i.e. Fig. 8. Since, in the Structural Model of Fig. 6, the dynamics of the inceptor are explicitly included in the model, it is important to at least approximate the dynamics of the inceptor. In the absence of a detailed nonlinear model of the collective, an approximate linear model was developed. Space does not permit a detailed description of the development of the linear representation, however on the basis of a computer simulation of a device with static and kinetic friction as shown in Fig. 8, the following linear model was developed:

$$Y_{FS} = \frac{1.0}{s(0.1s+1)} \quad \frac{applied\ force}{displacement} \qquad (2)$$

The particular units involved in Eq. 2 are not important here as the "gain" in the proprioceptive loop of the Structural Model is, in selected on the basis of the minimum damping ratio of any quadratic roots of the δ_M/E_M transfer function of Fig. 6 with all other loops open.

Previous efforts with an earlier incarnation of the Structural Model have been directed toward modeling the pilot with a variety of inceptors, including those without self-centering characteristics like the collective control used in this study.[9] It was found that matching measured pilot/vehicle transfer functions with such inceptors required a derivative element to be included in the neuromuscular system model. This derivative element will also be included here.

Choosing Pilot Model Parameters

References 4 and 8 provide detailed information about choosing the Structural Model parameters so that the crossover model of the human pilot[10] is in evidence. Pilot model parameter selection is straightforward. Only the results are presented here. Elements Y_{NM} and Y_{PF} are given by

$$Y_{NM} = \frac{\omega_{NM}^2 s}{s^2+2\zeta_{NM}\omega_{NM}s+\omega_{NM}^2} \qquad (3)$$

$$Y_{PF} = \begin{cases} K(s+a) & or, \\ K & or, \\ K/(s+a) \end{cases} \qquad (4)$$

with the particular equalization of Eq. 4 dependent upon the form of the vehicle dynamics, Y_c, around the crossover frequency. The zero at the origin in the neuromuscular system model of Eq. (3) is attributable to the nature of the inceptor, as has just been descrbied. The forms of the last of Eqs. 4 can be interpreted as the pilot's "internal model" of the vehicle dynamics. That is, in the range of crossover, $Y_{PF} \propto s \cdot Y_c(s)$. For reasons described in Refs. 4 and 8, a constant crossover frequency $\omega_c = 2.0\ rad/s$ is chosen.

A number of model parameters are considered invariant across different vehicles and tasks. Nominal values of these "fixed" parameters can be given as

$$\begin{aligned} \tau_0 &= 0.2\ s \\ \omega_{NM} &= 10\ rad/s \\ \zeta_{NM} &= 0.7 \end{aligned} \qquad (5)$$

The relatively simple relations of Eqs. 2-4 and the crossover relation $\omega_c = 2.0\ rad/s$ are all that are necessary to implement the model of Fig. 1. The selection of one of the three forms on the right hand side of Eq. 4 is done so that the resulting open loop transfer function

$$Y_p Y_c = \frac{\delta_M}{E}(j\omega)\cdot Y_c(j\omega) \approx \frac{\omega_c}{j\omega} e^{-\tau_e s} \quad for\ \omega \approx \omega_c \qquad (6)$$

i.e. $Y_p Y_c(j\omega)$ follows the dictates of the crossover model of the human pilot.[10] It is important to specify in a precise manner just how this is done. Limiting discussion to the last two forms of Y_{PF} (those most likely to be encountered in pilot/vehicle analyses), the right hand side of Eq. 4 is selected so that

$$\left| \frac{K}{Y_{PF}(j\omega)} \cdot Y_c(j\omega) \right| \approx \frac{K_1}{j\omega} \quad for \begin{cases} \omega \approx \omega_c \\ K_1\ arbitrary \end{cases} \qquad (7)$$

The gain K appearing in Eqs. 4 and 7 is chosen so that, with all other loops open, the minimum damping ratio of any quadratic closed-loop poles of $\frac{\delta_M}{E_M}(s)$ is $\zeta_{min} = 0.15$. Next, the vestibular loop is closed. This loop assumes that the time rate of change of the output of the primary control loop is amenable to sensing by the human vestibular system. The dynamics of a motion system such the washout dynamics of a flight simulator can be included in this loop. The gain $K_{\dot{m}}$ is chosen so that with all other loops open but the proprioceptive loop closed, the minimum damping ratio of any quadratic closed-loop

poles of $\frac{\delta_M}{E_M}(s)$ is $\zeta_{min} = 0.05$. Finally, K_e is selected so that the desired crossover frequency of 2.0 rad/s is obtained. The criteria for selecting K and $K_{\dot{m}}$ is based upon obtaining an open-loop pilot/vehicle transfer function $\frac{M}{E}(s)$ which exhibits, at least in an approximate sense, the high-frequency (10-15 rad/s) characteristics which have been measured in experiment.[10,11]

Model Overview

The pilot model of Fig. 6 establishes the framework within which analytical and experimental results will be interpreted. This model has been developed over a number of years and has been used, in one form or another, in a variety of pilot/vehicle analyses. In particular an earlier version of the model was used to hypothesize the manner in which the human pilot uses vestibular cues.[11] In the study of Ref. 11, it was demonstrated that a model of the human's use of motion cues could be presented that was a simple extension of that for static tracking, i.e., with no motion present. In terms of this model, motion does *not* provide fundamental compensation in tracking or regulation tasks, but rather serves to "tune" the pilot/vehicle dynamics by decreasing high-frequency phase lags occurring in the effective open-loop pilot/vehicle transfer function *after* the fundamental pilot compensation is accomplished through the proprioceptive loop closure. Figure 9 is a Bode plot of the pilot/vehicle transfer function M/E from Fig. 6 for the nominal vehicle, showing that the characteristics of the crossover model of the human pilot are in evidence.

Handling Qualities Sensitivity Functions

References 4 and 8 provide detailed information on how the Structural Model can be used to provide predictions of handling qualities. The levels of handling qualities are predicted on the Cooper-Harper scale of Fig. 3. Note that, as defined here, level 3 handling qualities extends to a Cooper-Harper rating of 10. The model-based metric which allows prediction of HQR and PIOR levels is the *Handling Qualities Sensitivity Function* defined as

$$HQSF \propto \left| \frac{U_M}{C}(j\omega) \right| \qquad (8)$$

Using flight-test handling qualities results, Ref. 4 demonstrated that the HQSF could be used to discriminate between handling qualities levels 1 - 3. Figure 10 shows the HQSF bounds which resulted from that study. The predicted handling qualities level for a particular aircraft was determined by the area in Fig. 10 which was penetrated by the HQSF when the pilot model was selected as described in the preceding.

Modeling Simulator Limitations

The technique for modeling simulator limitations was to first complete a pilot/vehicle analysis of a "nominal" vehicle. The "nominal" vehicle represents the vehicle dynamics as representative of the flight article as possible, i.e., not including any of the flight simulator limitations, here limited to variations in motion system characteristics and to time delays associated with the visual and motion system operation. The pilot model parameters thus chosen were then frozen and the simulator limitations introduced. Changes in the HQSF were then noted and compared with the HQSF of the nominal vehicle. Changes in these functions were then considered evidence of simulation fidelity problems. This technique is a refinement of that proposed in Ref. 2 and 3. *It should be emphasized that the resulting handling qualities predictions with simulator limitations are not indicative of those of the vehicle as simulated, since no attempt has been made to change the pilot model parameters from those obtained with the nominal vehicle model.*

Inverse Dynamic Analysis

It should be emphasized that the pilot/vehicle analysis to be undertaken will involve a computer simulation of the task using the computer-aided design program of Ref. 8. The pilot/vehicle system of Fig. 6 is clearly a compensatory one, i.e., error signals between command and output variables drive the system. While such compensatory structures are useful for tracking and regulation tasks, their face validity in the discrete bob-up/down maneuvers such as that being studied here is sometimes called into question. For example, in the past such tasks have been modeled by considering a precognitive *rapid-response* phase and followed by a compensatory *error-reduction* phase.[12,13]. While such a modeling approach is useful, it complicates the analysis of the maneuver using the handling qualities prediction technique described in the preceding. Using the

model of Fig. 7 with a 32-ft step input command, however, produces unrealistic tracking results unless nonlinear limiters are introduced at various points in the pilot model. Again, this complicates the analysis, and requires additional assumptions about the saturation values of the limiters. The compensatory structure of Fig. 7 can be retained, however, while still producing realistic results by appealing to inverse dynamic analysis.

The rationale behind using inverse dynamic analysis is that a compensatory structure can still be employed and produce performance comparable to that attained in flight or in pilot-in-the-loop simulation. The problem is approached by answering the following question: Using the compensatory structure of Fig. 7, what "command trajectory" $h_{com}(t)$ will produce an $h(t)$ which approximates that obtained in experiment? The answer can be found through inverse dynamic analysis. In the examples to be discussed, a distinction is made between "desired" and "command" trajectories. The "desired" trajectory is the one we wish the vehicle to follow in the task. The "command" trajectory is one actually employed in the computer simulation of the pilot/vehicle system and which forces the closed-loop *compensatory* pilot/vehicle system to produce the "desired" trajectory. Here, the command trajectory was obtained by the expedient of approximating the inverse of the closed-loop pilot/vehicle transfer function over a frequency range extending to approximately 10 rad/sec, a range more than adequate for creating an acceptable h_{com} Thus, the Laplace transform of the command trajectory ($h_{com}(s)$) was obtained as

$$h_{com}(s) = h_{des}(s) \cdot \frac{1}{\left[\frac{h}{h_c}(s)\right]_{approx}} \qquad (9)$$

where $h_{com}(s)$ is the "command" trajectory as just defined

$h_{des}(s)$ is the "desired" trajectory as just defined

$[h/h_c]_{approx}$ is a proper (as many poles as zeros) approximation to the h/h_c transfer function obtained from the compensatory pilot/vehicle system in Fig. 7, and valid up to a freuqency of 10 rad/s.

In implementing Eq. 9 it was typically necessary to include a pure prediction time, i.e., the inverse of a time delay. This prediction time typically was called into play to approximate the phase lag effects of right-half plane zeros of h/h_c when such zeros were replaced by symmetrical left-half plane zeros in $[h/h_c]_{approx}$. Implementing such a predictor in simulation was accomplished by the expedient of eliminating the predictor and simply delaying $h_{des}(t)$ by an equal amount.

The "desired" vehicle trajectory was defined here as

$$h_{des}(t) = \left(\frac{DISTANCE}{16}\right) \cdot \left[\cos\left(\frac{3 \cdot \pi \cdot t}{T_d}\right) - 9 \cdot \cos\left(\frac{\pi \cdot t}{T_d}\right) + 8\right] \quad m \qquad (10)$$

where *DISTANCE* refers to the required vertical translational distance of the bob-up/down maneuvers (32 ft)

T_d is the completion time of the maneuver, i.e, the first time instant at which $h_{des}(t) = DISTANCE$. Based upon the acceptable time-to-capture of Ref. 7, T_d was set to 6.5 s.

No desired trajectory such as that just created was included in the VMS simulation. The pilots were simply asked to meet the performance criteria of Table. 2. In the pilot/vehicle analysis, however, the trajectory of Eq. 10 resulted in smooth pilot model inputs with performance meeting the acceptable criteria of Table 2 with the nominal vehicle model.

Pilot Modeling Results

Bob-Up Maneuver Time Histories

The pilot modeling results will be presented in terms of a comparison of the HQSF plots for the

nominal vehicle and those of the vehicle as simulated in the VMS experiments. Only the bob-up maneuver will be discussed, as the modeling results are essentially identical for both bob-up and bob-down. Figures 11-14 show the results of the bob-up maneuver using the program of Ref. 8. Note in Fig. 11 how well the output of the compensatory pilot/vehicle system, $h(t)$, follows the h_{des} when h_{com} is applied to the pilot/vehicle system. Figure 14 is of particular interest as it compares the signals U_M (proprioceptive feedback) and U_S (vestibular feedback) in the Structural Model during the bob-up maneuver. Note that U_S is essentially an attenuated version of U_M. This will always be the case in the Structural Model since U_M will always be proportional to the rate of change of primary control loop output (here $\ddot{h}(t)$) due to pilot control inputs. In an inanimate controller, such redundancy would be unnecessary. In the human controller, however, the vestibular signal may serve as a tuning device for the proprioceptive dynamics Y_{PF}. We will have reason to return to the results of Fig. 14 when the fuzzy-inference identification results are discussed.

HQSF Comparison

Figures 15-19 show the HQSF for the nominal vehicle compared with that of each of the five motion configurations of Table 1. The shaded areas in each figure indicate the differences between the HQSF for the nominal vehicle and that of the simulated vehicle with simulator motion limitations. A metric based upon these area differences was defined as follows and is indicated on each of Figs. 15-19:

Normalized HQSF Metric for Config. "j" =

$$\frac{\int_0^{10} \left| [HQSF(\omega)]_j - [HQSF(\omega)]_{nom} \right| d\omega}{\min_{all\ j} \left[\int_0^{10} \left| [HQSF(\omega)]_j - [HQSF(\omega)]_{nom} \right| d\omega \right]} \qquad (11)$$

The bar graph of Fig. 20 compares these areas with those from the Average Composite Scores of Table 3 and a third metric yet to be described. As can be seen, the order of motion configurations from "most like" to "least like" the nominal in terms of area differences between HQSF's are V1, V13, V15, V14 and V10. This ranking is seen to agree with the pilot rating ranking obtained by numerically ordering the Average Composite Scores of Table 3. The caveat here is that there was no "nominal" configuration in the simulation study, i.e. even Config. V1 contained time delays from the visual and motion systems.[7] However, an estimate of the HQRs and PIORs for the nominal vehicle were obtained from the Structural Model results. These are shown in the last row of Table 3.

Fuzzy-Inference Identification Results

Introduction

Fuzzy set theory leads to a description of cause and effect relationships that differ considerably from control theoretic approaches in describing dynamic systems.[14] For example, in controlling the height of a rotorcraft in the stabilization mode of a bob-up maneuver, the pilot might define his/her control actions as follows:

If the height deviation is large and negative (below the target height) and the vertical velocity is also negative, my collective input is large and positive (i.e., commanding increased main rotor pitch).

or

If the height deviation is very small and negative and the vertical velocity is small and positive, my collective input is very small and negative

The "if-then" type of statements exemplified above are typical of fuzzy algorithms, as are use of fuzzy-conditional statements such as "very small". The fundamental idea in fuzzy systems is a generalization of the concept of a *set*. In classical set theory, there is a distinct difference between elements which belong to a set and those which do not. Fuzzy set theory allows elements to belong to more than one set, and assigns each element a membership value,

M, between 0 and 1 for each set of which it is a member.

Fuzzy-inference identification (FII) can be thought of as a means of generating membership functions and if-then rules so that the inputs to a dynamic system can be mapped into the output(s) with a high degree of precision, i.e., with little matching error. The numerical value of the inputs must be "fuzzified" to allow application of FII, then "defuzzified" to allow mapping into the numerical values of the estimated output. This process has been automated in computer-aided design packages such as the MATLAB Fuzzy Logic Toolbox.[15] As will be described, this toolbox was utilized in analyzing the behavior of three of the five pilots participating in the NASA VMS study. The advantages of FII are that no particular structure need be assumed for the system being identified, no special inputs are required, and nonlinearities pose no particular difficulty. The primary disadvantage of FII from a control theoretic standpoint, is that the models to which feedback control engineers are most accustomed, e.g., transfer functions, are not natural products of FII.

Interpreting Fuzzy-Inference Identification Results - The Surface View Plot

The if-then rules which result from FII can be graphically interpreted by means of surface view plots. Consider a system to be identified which has two inputs ($x_1(t)$, $x_2(t)$) and one output ($y(t)$). Next set x_2 equal to its most negative value obtained in the identification experiment. Then allow x_1 to vary across the range of values encountered in the experiment and allow the if-then rules to "fire", i.e., allow them to create the output values. Next x_2 is incremented and the procedure repeated. This process is continued until the most positive x_2 value is used. A three-dimensional surface view plot can now be created representing $y = f(x_1,x_2)$ an example of which is shown in Fig. 21. If more than two input variables are in evidence (as will be the case herein), surface view plots can still be obtained, however the remaining input variables are held constant, typically at their average values obtained in the identification experiment. Other constant values, however, can be chosen.

Fuzzy-Inference Identification and the Structural Pilot Model

The analytical framework provided by the Structural Model can also provide some guidance in interpreting the results of FII through surface view plots. In discussing the Structural Model, it has been hypothesized that the activity in the proprioceptive feedback loop determines the handling qualities level assigned to the vehicle and task. This proprioceptive activity can also be examined in FII through surface view plots. Referring to Fig. 6, δ_c and $\dot{h}(t)$ serve as x_1 and x_2 with δ_c also serving as y. δ_c is both a pilot input and output and the surface view is indicating how the variables on the horizontal axes (δ_c and $\dot{h}$) are contributing to the pilot output (δ_c) on the vertical axis.). If there is no activity in the proprioceptive control loop the resulting surface view plot should be planar and horizontal. In addition, according to the fundamental hypothesis invoked Ref. 4, the handling qualities will be optimum. This idea is identical to the *no tracking hypothesis* offered in Ref. 16: *"Optimum handling qualities demand minimum closed-loop control by the pilot"*. As will be seen, one possible experimental measure of the activity in the primary control loop would involve the geometry of the surface view plot just described, i.e., how much it differs from a horizontal planar surface.

Identification Results

Figure 22 shows the assumed pilot inputs and pilot output for the bob-up/down maneuvers. Figure 23 is a sample comparison of the collective time history from one of the bob-up maneuvers and the FII which resulted. The FII output is obtained by using the assumed pilot inputs of Fig. 22 from the VMS experiment as inputs to the identified fuzzy model of the pilot. The training parameter optimization for the FII was based on a hybrid procedure between least squares and back

propagation. The FII training was performed to bring the root-mean squar error between model and pilot output to $1 \cdot 10^{-5}$. All the FII results were of this quality. As an example of the nature of the surface view plots, Fig. 24 shows results for a single bob-up and bob-down maneuver for Pilot A for Config. V1.

Since three repetitions of the two separate maneuvers (bob-up and bob-down) were utilized in the experiment, some means of "averaging" these was necessary to obtain a single metric for comparison with handling qualities, etc. The following metric was created:

$$\textit{Avg. Norm. Surface View Metric for Config. "j"} = \frac{\sum_{all\ pilots}\left[\sum_{i=1}^{3}(V_{BU_i})_j+\sum_{i=1}^{3}(V_{BD_i})_j\right]}{\min_{all\ j}\left\{\sum_{all\ pilots}\left[\sum_{i=1}^{3}(V_{BU_i})_j+\sum_{i=1}^{3}(V_{BD_i})_j\right]\right\}} \quad \textbf{(12)}$$

where

V_{BU_i} represents the volume above minimum vertical coordinate on the Surface View plot for the "ith" bob-up

B_{BD_i} represents the volume above the minimum vertical coordinate on the Surface View plot for the "ith" bob-down

$\min_{all\ j}$ represents the minimum sum of the volumes for all configurations and pilots

In calculating the volumes as prescribed by Eq. 12, care needs to be taken in interpreting volumes as a measure of control activity. For a case in which a restrained manipulator is being used, e.g., a self-centering control stick, the volumes in Eq. 12 should be calculated with the "trim" manipulator position as the datum. The total volume above and below the horizontal plane defined by this datum value would be used in calculating the volumes in Eq. 12. In the case of the "unrestrained" collective inceptor used in the VMS simulation, where no self-centering characteristics are in evidence, one is left with either using an average position over the maneuver as the datum, or as was done here, defining the datum as the most negative collective input. This was feasible here since, in the bob-down maneuver, the collective, vertical velocity and vertical acceleration signals were modified so that the surface view plots could be compared to those in the bob-up maneuver. For the bob-down maneuver, these modifications were

$$\begin{aligned} (\textit{vert accel})_{\text{mod}} &= -(\textit{vert accel}) - 64\ \textit{ft/s}^2 \\ (\textit{collective})_{\text{mod}} &= 11 - \textit{collective in} \\ (\textit{vert vel})_{\textit{down}} &= -(\textit{vert vel})\ \textit{ft/s} \end{aligned} \quad \textbf{(13)}$$

Also, the remaining input variables not included on the surface view plot, i.e., height error and vertical acceleration (for all but Config. V10) were set to values representing the terminal part of the maneuver.

The last column of Table 3 represents the Average Normalized Surface View Metric (SVM) calculated as given in Eq. 12. The bar graph of Fig. 20 compares the Average Normalized SVM and the Average Composite Scores. The order of the motion configurations from "most like" to "least like" the nominal is seen to be V1, V13, V15, V14 and V10. One sees that the ordering of the last two configurations differs from that established with the Average Composite Scores. Nonetheless, the results are noteworthy. Metrics other than Eq. 12 can be employed, of course. The metric of Eq. 12 was chosen because of its relation to activity in the assumed primary control loop in the bob-up/down maneuvers. Obviously more research in this area is warranted.

Discussion

One important hypothesis regarding pilot utilization of proprioceptive and vestibular cues can be advanced based upon the research described

herein. Namely that in a control-theoretic sense both the vestibular and proprioceptive feedback signals provide redundant information. However, the vestibular feedback may be of higher quality, with a broader bandwidth than that obtainable from proprioceptors. In this light, the vestibular feedback may serve to "tune" the dynamics of the proprioceptive feedback loop in addition to decreasing phase lags in the transfer function of the open-loop pilot/vehicle system. When the quality of the vestibular information is degraded from "nominal", the fuzzy-inference identification clearly shows an increase in proprioceptive activity which also has been hypothesized to be a harbinger of degraded handling qualities.[4] Degradations in handling qualities were indeed noted in the pilot ratings from the simulation experiment when the motion system characteristics were degraded through either gain reduction or washout dynamics.

The results presented have been limited to a single-axis control task. Extension of the results to multi-axis tasks is an obvious prerequisite to the practical evaluation of simulator fidelity. Research is continuing in this area.

Conclusions

An analytical and experimental investigation of the manner in which pilots perceive and utilize visual, proprioceptive and vestibular cues in a ground based flight simulator led to the development of a pair of metrics which were used to assess simulator fidelity.

(1) The analytical approach used an established pilot/vehicle analysis technique based upon a Structural Model of the pilot from which was obtained Handling Qualities Sensitivity Functions. A metric based upon area differences between the Sensitivity Functions for the nominal and simulated pilot/vehicle system were shown to correlate well with composite rating scores obtained from a simulation experiment conducted on the NASA Ames Vertical Motion Simulator.

(2) Fuzzy-inference identification was exercised using the NASA simulation data for three pilots. A total of 90 separate identification were completed. After identifying the "fuzzy pilot models" for each pilot, surface view plots were obtained which graphically displayed the results of the identification. A metric based upon the geometry of these plots was also shown to correlate well with the composite rating scores obtained from the experiment.

(3) Further research is warranted in extending this methodology to multi-axis tasks, and in refining the fidelity metric used in the fuzzy-inference identification results.

References

[1]Atencio, A. Jr., "Fidelity Assessment of a UH-60A Simulation on the NASA Ames Vertical Motion Simulator,' NASA TM 104016, 1993, NASA Ames Research Center, Moffett Field, CA.

[2]Hess, R. A. and Malsbury, T., "Closed-Loop Assessment of Flight Simulator Fidelity," *Journal of Guidance, Control and Dynamics*, Vol. 14, No. 1, 1991.

[3]Hess, R. A., Malsbury, T., and Atencio, A., Jr., Flight Simulator Fidelity Assessment in a Rotorcraft Lateral Translation Maneuver," *Journal of Guidance, Control and Dynamics*, Vol. 16, No. 1, 1993.

[4]Hess, R. A., "Unified Theory for Aircraft Handling Qualities and Adverse Aircraft-Pilot Coupling," *Journal of Guidance, Control and Dynamics*, Vol. 20, No. 6, 1997.

[5]Kramer, U., and Rohr, G., "A Model of Driver Behavior," *Ergonomics*, Vol. 25, No. 10, 1982.

[6]Wu, J. C., and Liu, T. S., "A Fuzzy Model of Rider Control for a Motorcycle Undergoing Lange Change," *International Journal of Vehicle Design*, Vol. 15, Nos. 1/2, 1994.

[7]Schroeder, J. A., Chung, W. W. Y., and Hess, R. A., "Spatial Frequency and Platform Motion Effects on Helicopter Altitude Control," AIAA Paper No. 99-4113, 1999.

[8]Zeyada, Y., and Hess, R. A., "PVD_{NL}, Pilot/Vehicle Dynamics $_{NonLinear}$, An Interactive Computer Program for Modeling the Human Pilot in Single-Axis Linear and Nonlinear Tracking Tasks," Dept. of Mechanical and Aeronautical Engineering, University of California, Davis, CA, 1998.

[9]Hess, R. A., Analyzing Manipulator and Feel system Effects in Aircraft Flight Control," *IEEE Transactions on Systems, Man, and Cybernetics,* Vol. 20, No. 4, 1990, pp. 923-931.

[10]Hess, R. A., "Feedback Control Models - Manual Control and Tracking," in *Handbook of Human Factors and Ergonomics, 2nd Ed.*, Ed: G. Salvendy, Wile, New York, 1997, to appear.

[11]Hess, R. A., "Model for Human Use of Motion Cues in Vehicular Control," *Journal of Guidance, Control, and Dynamics,* Vol. 13, No. 3, 1990, pp. 476-482.

[12]Ferguson, S. W., Clement, W. F., Cleveland, W. B., and Key, D. L., "Assessment of Simulation Fidelity Using Measurements of Piloting Technique in Flight," American Helicopter Society, Paper A-84-40-08-4000, May 1984.

[13]Ferguson, S. W., Clement, W. F., Hoh, R. H., and Cleveland, W. B., "Assessment of Simulation Fidelity Using Measurements of Piloting Technique in Flight, Part II," American Helicopter Society, 41st Annual American Helicopter Society Forum, May 1985.

[14]Zadeh, L. A., "Outline of a New Approach to the Analysis of Complex Systems and Decision Processes," *IEEE Transactions on Systems, Man, and Cybernetics,* Vol. SMC-3, No. 11, 1973, pp. 28-44.

[15]Anon, *Fuzzy Logic Toolbox for Use with MATLAB, User's Guide*, The MathWorks, Inc., Natick, MA, 1998.

[16]Smith, R. E., and Geddes, N., "Handling Qualities Requirements for Advanced Aircraft Design: Longitudinal Mode," AFFDL-TR-78-154, Air Force Flight Dynamics Lab, Wright-Patterson AFB, OH, Aug. 1979.

Table 1 Vehicle Dynamics and Motion Configurations

Vehicle Dynamics

$$\dot{x}(t) = Ax(t) + Bu(t)$$

$$A = \begin{bmatrix} -0.122 & -118 \\ 0 & -12.9 \end{bmatrix} \qquad B = \begin{bmatrix} 14.6 \\ 1 \end{bmatrix}$$

$$x(t) = [\dot{h}(t) \quad z(t)]^T$$

$$u(t) = \delta_C(t-0.15)$$

$\dot{h}(t)$ = *vertical velocity ft/s*

$z(t)$ = *dynamic inflow parameter* ft/s^2

$\delta_C(t)$ = *collective displacement in*

An additional 0.12 s time delay included in visual and motion channels in pilot/vehicle analyis to account for VMS delays.[7]

Motion Configurations

Configuration	$\ddot{h}_{motion}/\ddot{h}_{command}$
V1	1.0
V10	0
V13	0.5
V14	$\frac{0.5s^2}{s^2+2(0.707)0.521s+0.521^2}$
V15	$\frac{0.5s^2}{s^2+2(0.707)0.885s+0.885^2}$

Table 2 Task Performance Standards

Segment	Desired	Adequate
Ascent	< 6 s	< 10 s
10 s at top	± 2 ft	± 5 ft
Descent	< 6 s	< 10 s
10 s at bottom	± 2 ft	± 5 ft

Table 3 Pilot Rating and Fuzzy Inference Identification Summary

Pilot	Config	HQR A,B,C	PIOR A,B,C	MFR A,B,C	Average Composite Score	Average Normalized SVM
	V1	3,2,3	1,1,2	2,3,2	1.00	1.0
	V10	5,4,4	5,3,3	1,1,1	2.19	2.27
	V13	4,3,2	4,2,2	2,3,3	1.21	1.28
	V14	5,5,4	4,3,4	2,2,2	1.69	2.39
	V15	4,4,3	2,2,3	2,3,2	1.28	2.09
	nominal	3,3,3[a]	2,2,2[a]	∞,∞,∞	0.54	

[a] nominal vehicle HQRs and PIORs estimated from Structural Model results

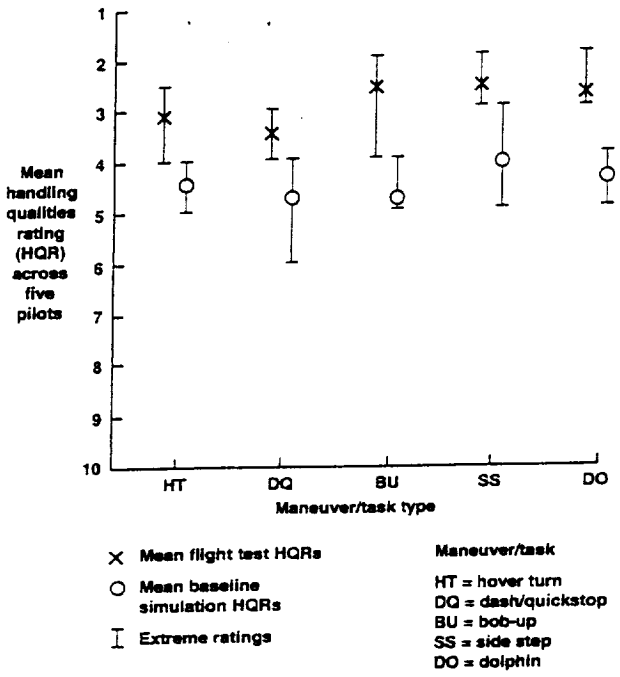

Fig. 1 A simulator fidelity problem from Ref. 1

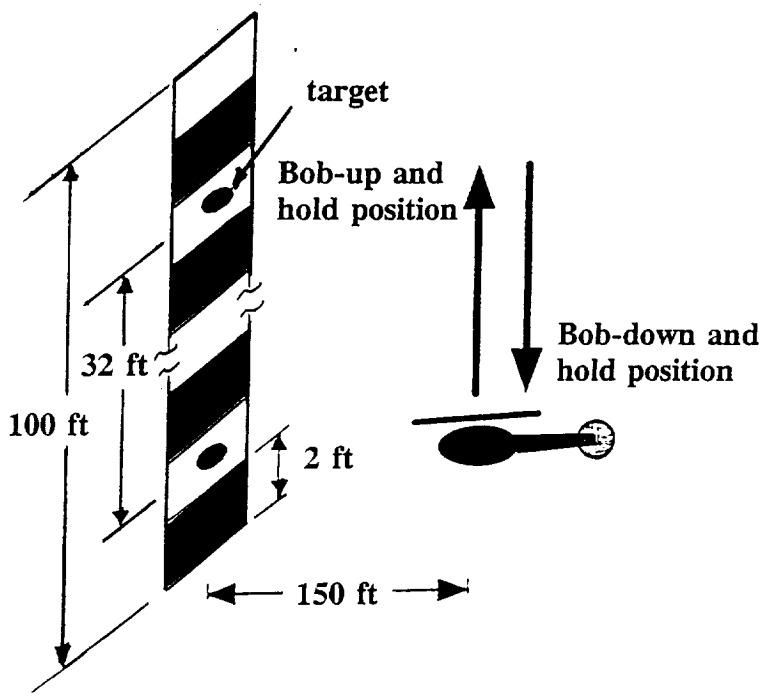

Fig. 2 The NASA VMS task geometry

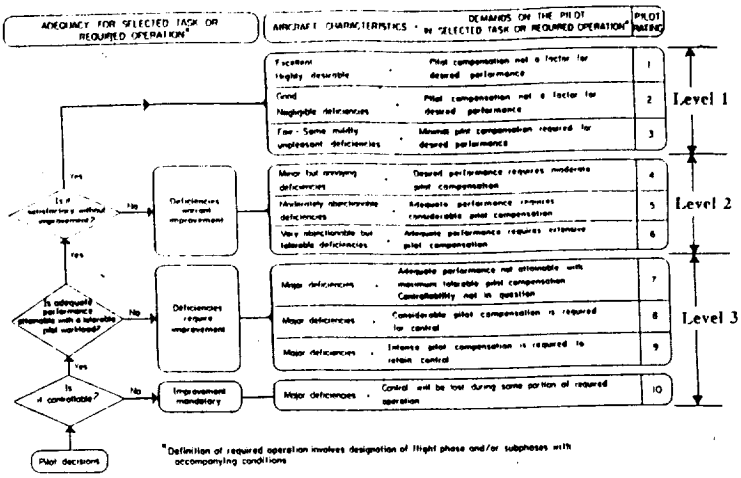

Fig. 3 The Cooper-Harper rating scale

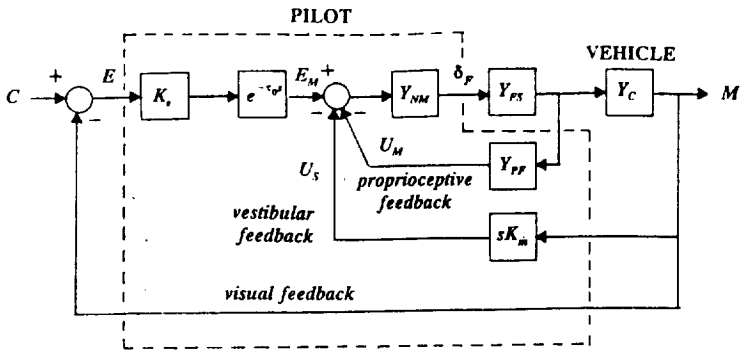

Fig. 6 The Structural Model of the human pilot

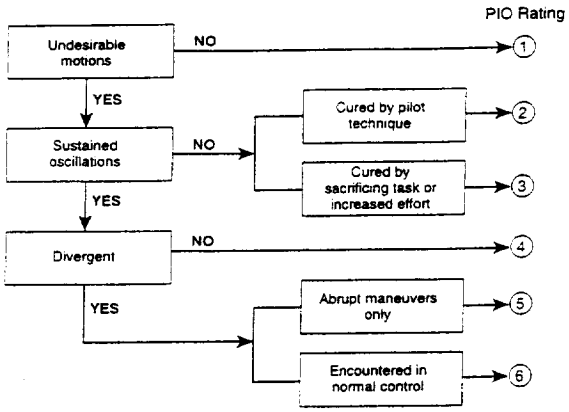

Fig. 4 The PIO rating scale

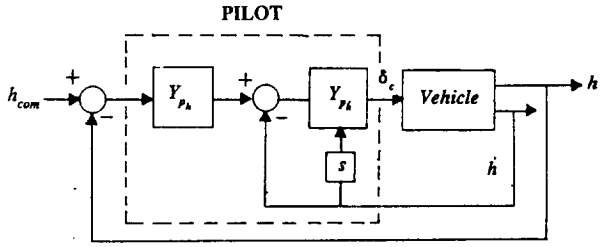

Fig. 7 The hypothesized pilot/vehicle system for the bob-up/down maneuvers

Motion Fidelity Scale

Fidelity Rating	Definition	Numerical Rating[a]
High	Motion sensations like those of flight	3
Medium	Motion sensations are noticeably different from flight, but not objectionable	2
Low	Motion sensations are noticeably different from flight and objectionable	1

[a] Numerical rating assigned for purposes of analysis.

Fig. 5 The Motion Fidelity Scale from Ref. 7

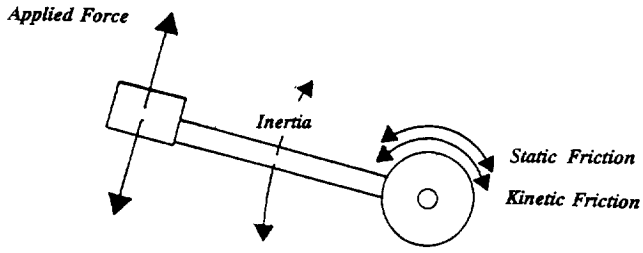

Fig. 8 The collective inceptor

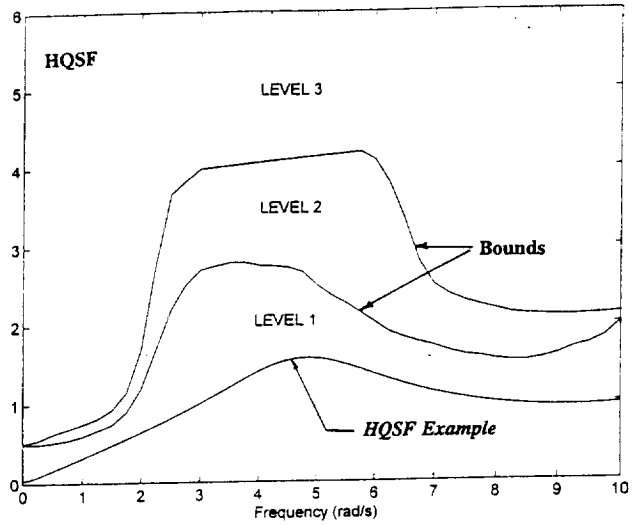

Fig. 9 The HQSF bounds for predicting handling qualities levels

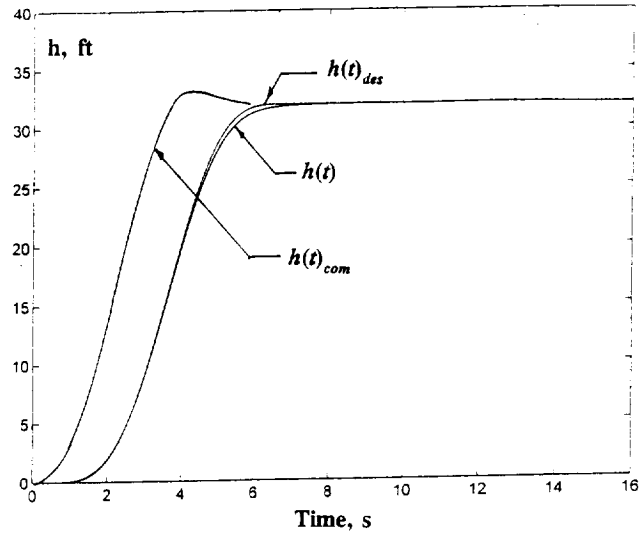

Fig. 11 The height desired, height commanded and height response of the simulated pilot/vehicle system

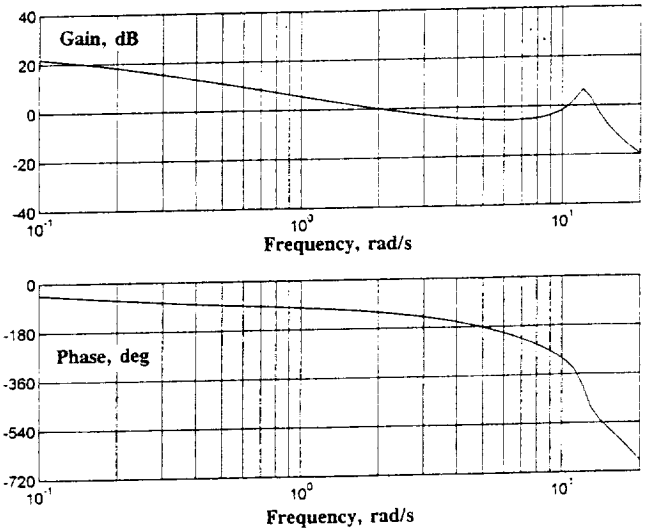

Fig. 10 The Bode diagram of the open-loop pilot/vehicle system for nominal configuration

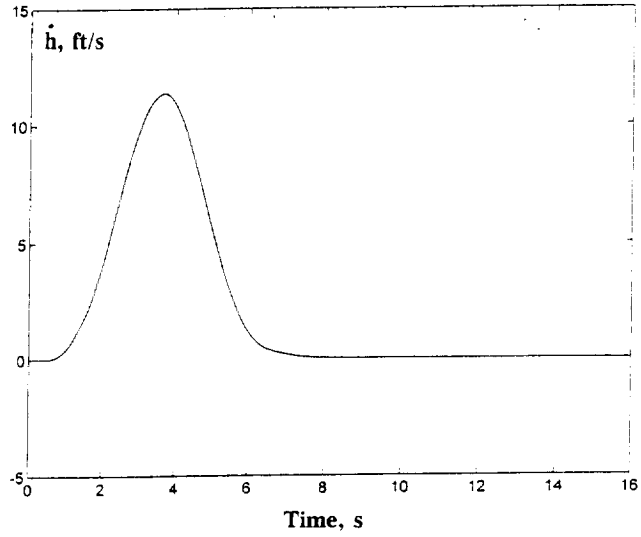

Fig. 12 The vertical velocity response of the simulated pilot/vehicle system

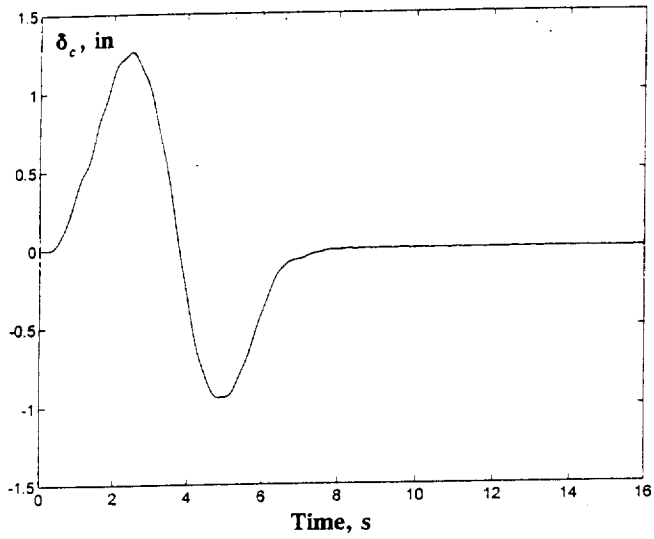

Fig. 13 The collective input in the simulated pilot/vehicle system

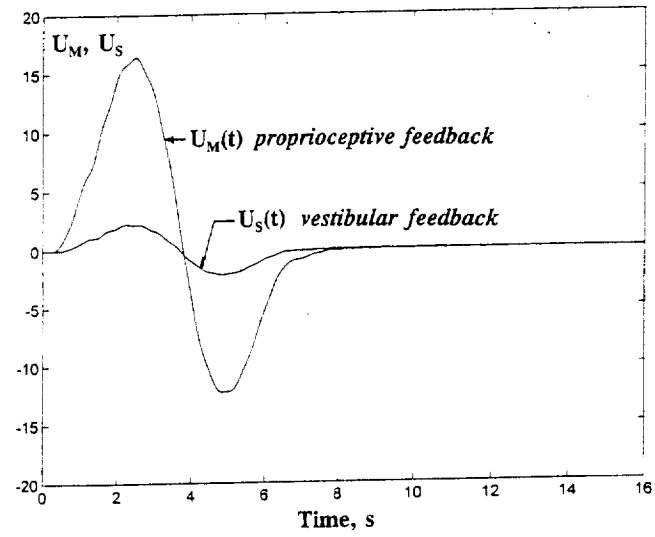

Fig. 14 The proprioceptive and vestibular signals in the simulated pilot/vehicle system

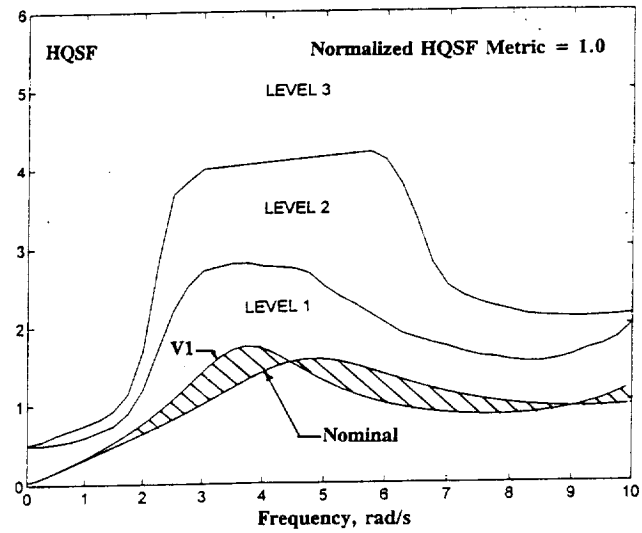

Fig. 15 The HQSF comparisons for nominal and V1 configurations

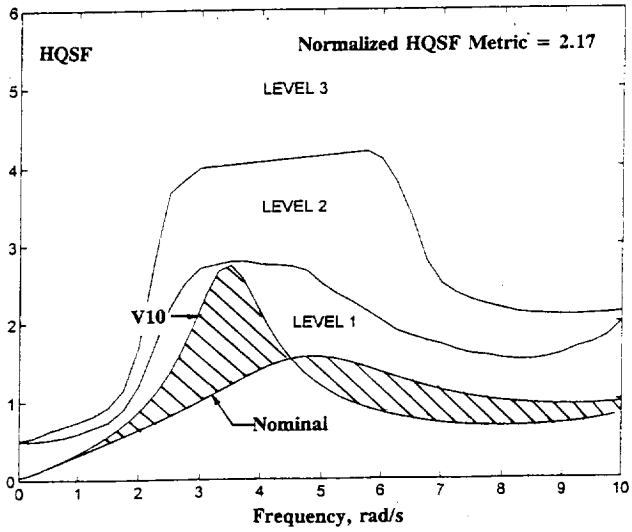

Fig. 16 The HQSF comparisons for nominal and V10 configurations

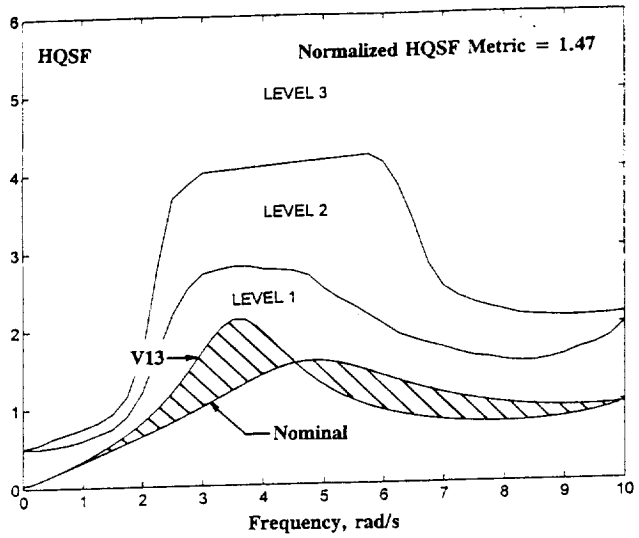

Fig. 17 The HQSF comparisons for nominal and V13 configurations

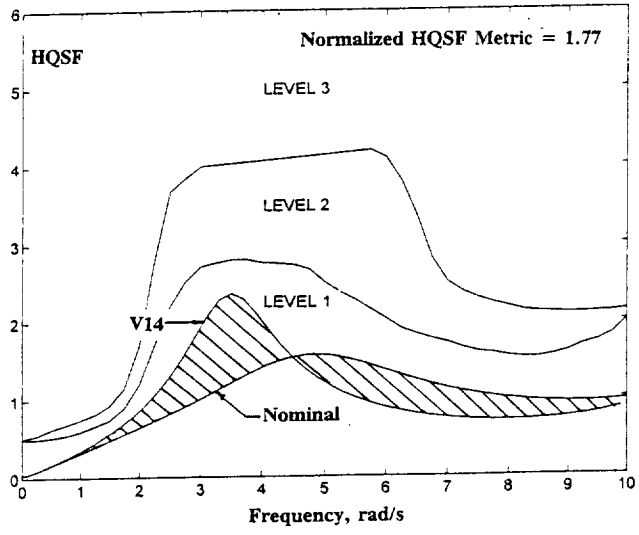

Fig. 18 The HQSF comparisons for nominal and V14 configurations

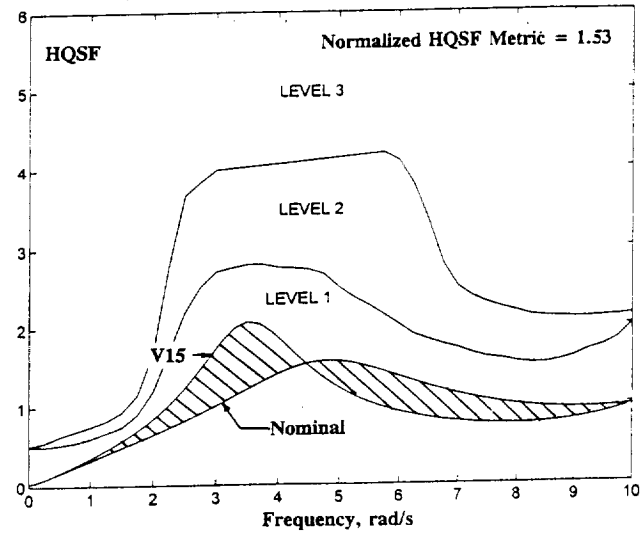

Fig. 19 The HQSF comparisons for nominal and V15 configurations

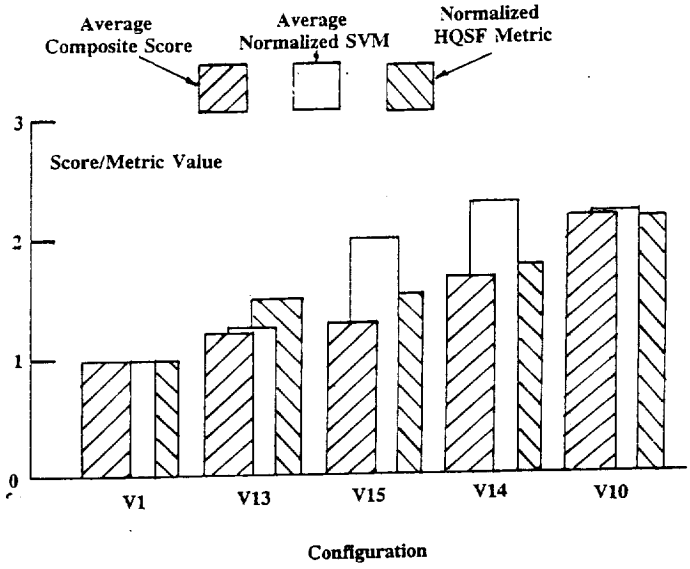

Fig. 20 A bar graph comparison of experimental and analytical results

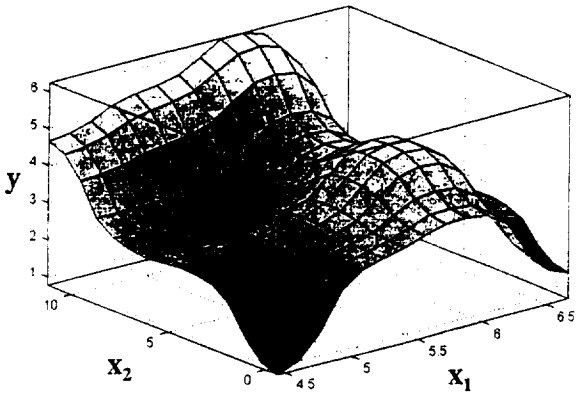

Fig. 21 A surface view plot

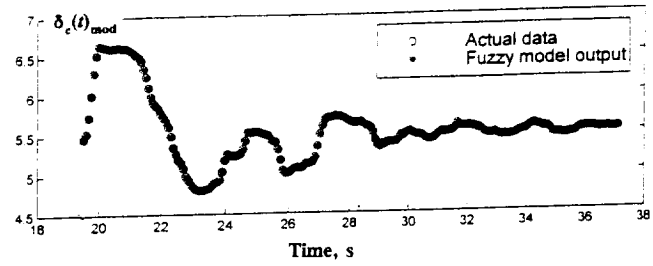

Fig. 23 An example of fuzzy inference identification: comparing collective time histories from experiment and identified fuzzy pilot model

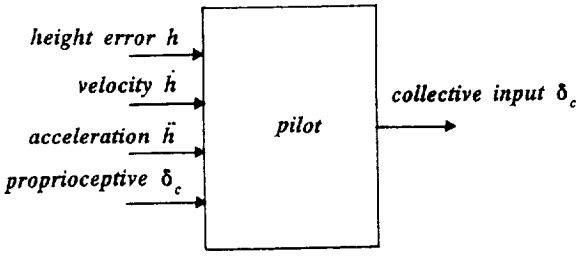

Fig. 22 The hypothesized pilot inputs and output for fuzzy-inference identification in the bob-up/down maneuvers

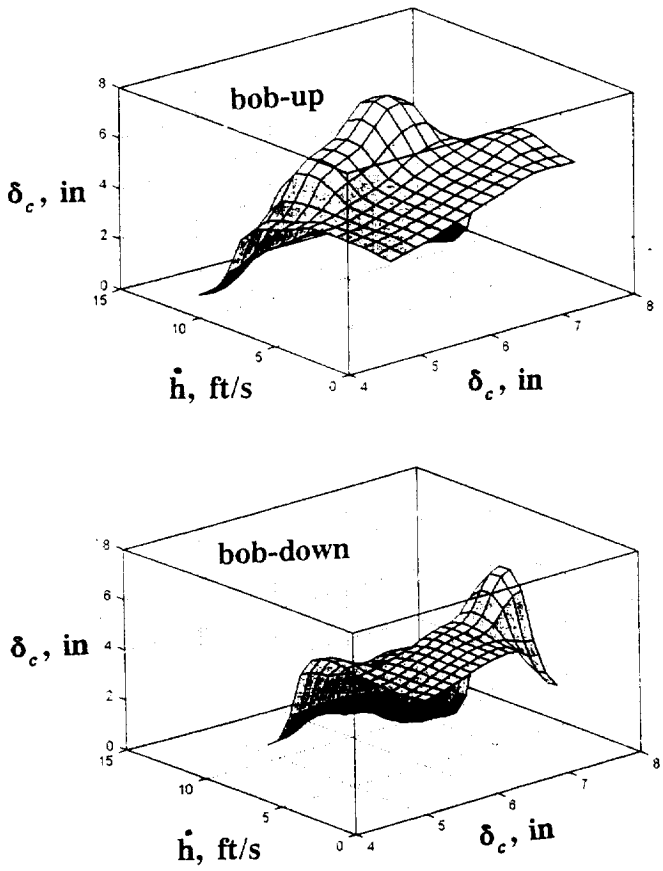

Fig. 24 Surface view plots for bob-up and bob-down maneuver; Pilot A, Config. V1